論文80-17-6-3

Field Analysis of Surface Acoustic Wave Transducers
(表面波 트랜스듀서의 電磁理論的 分析)

康 昌 彦*
(Kang Chang E.)

要 約

表面波 전자기구의 送受信特性을 단극, 이극, 삼극, 트랜스듀서의 例를 들므로써 理論的으로 分析하였다. 電磁氣 理論에 依한 出力信号를 誘導하였으며 基本分析方法은 一般的으로 널리 모든 유형의 表面波기구에도 이용될 수 있음을 보이고 있다. 理論的으로 장단점을 이해하고 결론적으로 광범위한 응용을 전제하고 있다.

Abstract

The transmission and reception characteristics of surface acoustic wave devices are analyzed by introducing three different types of transducers, such as single-electrode transducer, double-electrode transducer and triple-electrode transducer. Utilizing an electromagnetic field theory technique, the output signal has been derived theoretically. The basic analysis used here can be extended for other configurations. The surface acoustic devices have been shown promising as a means of improving the operation efficiency by modifying the geometric configuration of transducer strips.

Introduction

The analysis of surface acoustic wave (SAW) generation and transmission has been a central problem in SAW technology since 1965 (1), (2) when White and Voltmer demonstrated efficient SAW transduction by interdigital transducers (3). Auld analyzed the SAW phenomena theoretically in a variety of ways (2). Ever since, SAW devices have been finding applications as delay lines, filters, digital coding and holographic imaging in medicine, detection of underwater objects, pulse compressors, pressure transducers, and signal processing functions in radar, navigation, electronic counter measures and communication systems (4), (5), (6), (7), (8), (9), (10). Extensive research has been given to analyze the characteristics of interdigital transducers for efficient applications by several workers (11), (12), (13), (14). Recently, Kang analyzed SAW resonators by electromagnetic field theory (10).

Various application of SAW devices has been accelerated by the demand of the electronics industry. Commercially, band pass filters for AM and FM receivers, delay lines which for example, 64 micro seconds delay line in European color TV set, American TV IF filters, ultrasonic propagation in water such as depth-finders and fish-finders, and digital recirculating memories are undergoing concentrated development. In SAW devices, the wave is mainly propagated on the crystal surface while in bulk acoustic devices the signal is propagated through the bulk of the material. The electric signal of input transducer, in both cases, is converted to the acoustic wave by mechanical deformation. The acoustic wave is propagated along the active length of the device which is in between the

*正會員, 북일리노이 주립대학교
(Northern Illinois Univ.)
接受日字 : 1980年 5月 12日

input and output transducer, and is reconverted to the electric signal at the output transducer.

The primary components involved with these energy conversion are the transducers, and the geometrical configuration of transducers determines frequency selectivity of surface wave filters. Electromagnetic field theory is applied to analyze the wave characteristics of various transducers, and to understand the energy conversion scheme from the electric signal to acoustic signal, or the acoustic signal to electric signal. The transmission and reception of the signal depend upon the number of strips of transducers and geometric configuration of strips. It is assumed that there is no attenuation on the crystal surface, interactions between input and output transducers, and energy conversion loss.

The output signal of the transducer is calculated by adding all electric fields over all strips of the transducer. Three different types of transducer are investigated for the analytical purpose, i.e., single-electrode transducer, double-electrode transducer and triple-electrode transducer. Design criteria can be obtained by the theoretical analysis.

Single-electrode Transducer

A single-electrode transducer which generates SAW is shown in Fig. 1.

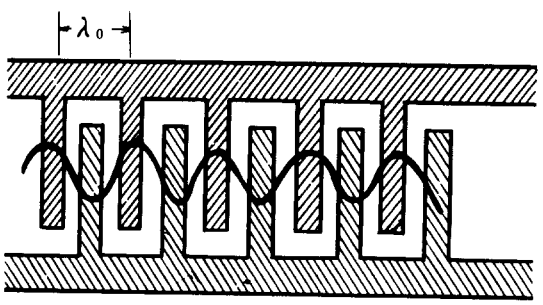

Fig. 1. Single-electrode transducer configuration.

The optimum frequency f_0 which gives maximum surface energy is obtained by

$$f_0 = \frac{v}{\lambda_0} \tag{1}$$

where v = acoustic surface wave velocity and

λ_0 = period of the pitch (or wavelength of the acoustic wave)

The surface wave velocity in Y cut $LiNbO_3$ is $v = 3.4 \times 10^5$ cm/sec.

The transducer is analogous to antenna array which has a definite directivity and therefore the frequency selectivity of the transducer can be obtained by the antenna analog. There is n half wavelength strips in the transducer and take the first strip as a reference. Then the progressive phase shift ψ_n may be obtained.

$$\psi_0 = 0 \tag{2}$$

where ψ_0 is the phase shift of the first strip. The total phase shift in the second strip becomes

$$\psi_1 = \beta d \cos\phi + \alpha \tag{3}$$

where β = wave propagation constant

d = distance between two strips

ϕ = vertical pattern angle when the direction of the output transducer is taken as 0°.

α = phase angle of currents between two strips

ψ_1 can be written in terms of prequency as

$$\psi_1 = \beta\frac{\lambda_0}{2}\cos\phi + \alpha = \frac{\omega}{2f_0}\cos\phi + \pi \tag{4}$$

The angle π between two strips arises from the fact that alternate strips of the transducer are connected to the input excitation with different polarity.

Similarly,

$$\psi_2 = \frac{\omega}{f_0}\cos\phi + 2\pi \tag{5}$$

$$\vdots \quad \vdots \quad \vdots$$

$$\psi_{n-1} = \frac{n-1}{2}\frac{\omega}{f_0}\cos\phi + (n-1)\pi \tag{6}$$

Introducing the frequency of input signal f close to f_0, the frequency departure

$$\Delta f = f - f_0 \tag{7}$$

Using Eq. (7), and Eqs. (4) through (6) may be rewritten as

$$\psi_1 = \pi(1 + \frac{\Delta f}{f_0})\cos\phi + \pi \tag{4}'$$

$$\psi_2 = 2\pi(1 + \frac{\Delta f}{f_0})\cos\phi \tag{5}'$$

$$\psi_{n-1} = 2(n-1)\pi(1 + \frac{\Delta f}{f_0})\cos\phi + (n-1)\pi \tag{6}'$$

Let E_0 be maximum electric field intensity from the first strip of the transducer. The total output electric

field intensity is obtained by

$$\vec{E} = \vec{E}_0(1 + e^{j\psi_1} + e^{j\psi_2} + \cdots + e^{j\psi_{n-1}}$$

$$= \vec{E}_0 \frac{1 + e^{jn\pi\gamma}}{1 + e^{j\pi\gamma}} \tag{8}$$

where $\sigma = (1 + \Delta f/f_0)\cos\phi$

$$\text{or } \vec{E} = \vec{E}_0 e^{j\pi(n-1)\gamma} \frac{\cos(n\pi\gamma/2)}{\cos(\pi\gamma/2)} \tag{9}$$

the output electric field intensity in the direction of propagation is, at $\phi = 0$,

$$\vec{E} = \vec{E}_0 e^{\frac{j\pi\Delta f(n-1)}{f_0}} \cdot \frac{\sin\frac{n\pi\Delta f}{2f_0}}{\sin\frac{\pi\Delta f}{2f_0}} \tag{10}$$

Since, if $\Delta f \ll f_0$, $\sin\frac{\pi\Delta f}{f_0} = \frac{\pi\Delta f}{f_0}$ and then

$$\vec{E} \simeq n\vec{E}_0 e^{j\pi\Delta f(n-1)/f_0} \cdot \frac{\sin(n\pi\Delta f/2f_0)}{(n\pi\Delta f/2f_0)} \tag{10-a}$$

Eq. (10) indicates that output response is of the $\frac{\sin nx}{\sin x}$ or $\frac{\sin x}{x}$ form and is a function of the propagation angle. It can be seen that from Eq. (9) depending on the direction, there are a transmitted wave into the output transducer, a penetrating wave into the crystal (or penetration loss and a radiation loss. On the way of wave penetration into the crystal, some reflection may arise on the surface of the transducer area.

(a) Transmitted wave in the direction of propagation.

To calculate the wave transmitted to the direction of the output transducer, Eq. (10) is used. The magnitude of E is then

$$E \simeq \left| \frac{\sin\frac{n\pi\Delta f}{2f_0}}{\sin\frac{n\pi\Delta f}{2f_0}} \right| \tag{11}$$

or

$$E \simeq nE_0 \left| \frac{\sin\frac{n\pi\Delta f}{2f_0}}{\frac{n\pi\Delta f}{2f_0}} \right| \tag{12}$$

The output response can be plotted to see frequency selectivity shown in Fig. 2.

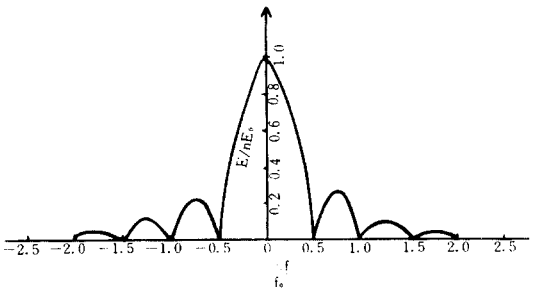

Fig. 2. Frequency selectivity for n = 4.

In Fig. 2, one can easily deduce that for large n, all E components close at a small frequency departure Δf, so that the bandwidth is inversely proportional to n. It can be seen clearly by sketching the output response for n=20 shown in Fig. 3.

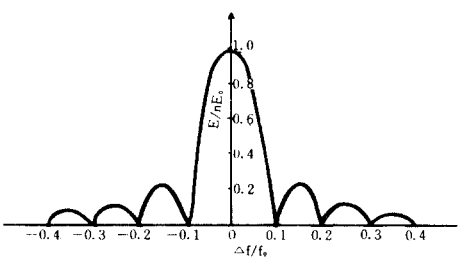

Fig. 3. Frequency selectivity for n = 20.

For large n,

$$\lim_{\Delta f \to 0} \frac{\sin\frac{n\pi\Delta f}{2f_0}}{\sin\frac{\pi\Delta f}{2f_0}} = n \tag{13}$$

$$\lim_{\frac{\pi\Delta f}{f_0} \to \frac{2\pi k}{n}} \frac{\sin\frac{n\pi\Delta f}{2f_0}}{\sin\frac{\pi\Delta f}{2f_0}} = 0 \qquad k = 1,2,3,\cdots \tag{14}$$

and the first maximum occurs at $\frac{\pi\Delta f}{f_0} = \frac{3\pi}{n}$. The maximum amplitude is obtained as

$$\left. \sin\frac{n\pi\Delta f}{2f_0} \middle/ \sin\frac{\pi\Delta f}{2f_0} \right|_{\frac{\pi\Delta f}{2f_0} = \frac{3\pi}{n}} = \frac{2\pi}{3\pi} \tag{15}$$

From Eq. (14), the first null occurs at

$$\frac{\pi\Delta f}{f_0} = \frac{2\pi}{n}$$

or

$$\Delta f = \frac{f_0}{n/2} \tag{16}$$

From Eq. (15), the amplitude of the principal maximum was n, so the amplitude ratio of the first secondary maximum to principal maximum is $\frac{2}{3} = 0.2/2$. This means that the first secondary maximum is about 13.5 db below the principal maximum and this ratio is independent of the number of stripes in the circuit, as long as the number is large.

When $(n\pi\Delta f/2f_0) = \frac{\pi}{2}$

$$E = E_0 \frac{1}{n\pi\Delta f/2f_0} = \frac{\pi}{2}E_0 = 0.03\,E_0 \tag{17}$$

The bandwidth are measured between the first nulls and is twice the angle, then, from Eq. (16).

$$BW = 2\Delta f = \frac{4f_0}{n} \tag{18}$$

It is mathematically confirmed that the bandwidth is inversely proportional to n, number of strips. For instance, a surface wave device for n=30 and f_0=15 MHZ may be disigned as

(a) Nulls: $\frac{\pi\Delta f}{f_0} = \frac{2\pi k}{n}$, $k = 1,2,3,4,\cdots$

$$\Delta f = \frac{2f_0 k}{n} = 10^6 k$$

(b) $f = f_0 + Cf = 12, 13, 14, \underline{15}, 16, 17, 18, \cdots$ MHZ

(c) $BW = \frac{4f_0}{n} = 2$ MHZ

The output response for this example is plotted in Fig. 4.

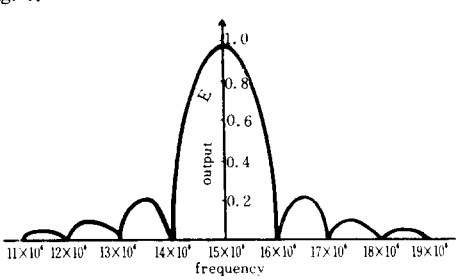

Fig. 4. Output Response at f_0 = 15 MHZ and n = 30.

The main lobe of the response can be used as a band pass region and the side lobes of large attenuation as traps. The design of the surface wave device depends on number of strips n and on the distance ℓ between input and output transducers.

The time delay between input and output transducer is

$$\tau = \frac{\ell}{v} \tag{19}$$

Since $f\tau$ = constant, $\frac{f}{\Delta f}$ may be written in terms of the delay time τ as

$$f\Delta\tau + \tau\Delta f = 0$$

or

$$\frac{f}{\Delta f} = -\frac{\tau}{\Delta\tau} \tag{20}$$

It is noted that the wave is not only propagated in the direction of receiver but also in the opposite direction of receiver. To receive the signal effectively, reflectors are usually used in the opposite direction (17).

(b) Wave propagation under the surface

As one can see from Eq. (9), there is an unwanted wave propagation under the surface of crystal in the range of $0 < \phi < 180°$. This wave undergoes down to the surface first time and splits into two components. One component decays with the depth of crystal and approaches zero, and another component radiates on the surface depending on the material property.

These components are varied with the number of strips, applied frequency and the propagation angle. The loss due to such effect may be calculated by squaring the E field pattern from ϕ=0° to ϕ=180°.

(c) Wave Propagation normal to the surface

This component of propagation field is traveling above the crystal in the range of $180° < \phi < 360°$. The traveling wave in this range constitutes mainly a radiation loss. Note that the cases (b) and (c) are not any more surface waves.

Double-electrode Transducer

A double-electrode transducer is shown in Fig. 5, which each finger strip is split into two electrically interconnected strips.

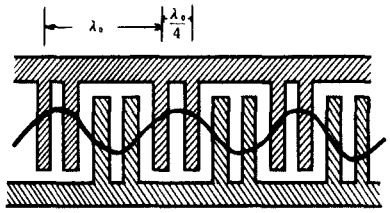

Fig. 5. Double-electrode transducer configuration.

Similar to the single-electrode transducer, the progressive phase shift ψ_n for each strip becomes

$$\psi_0 = 0 \tag{21}$$

$$\psi_1 = \beta d\cos\phi + \alpha = \frac{\omega}{v}\frac{\lambda_0}{4}\cos\phi + 0 = \frac{\pi}{2}\gamma \tag{22}$$

$$\psi_2 = 2\beta d\cos\phi + \alpha = \pi(\gamma + 1) \tag{23}$$

$$\psi_3 = 3\beta d\cos\phi + \alpha = \pi(\frac{3}{2}\gamma + 1) \tag{24}$$

$$\psi_4 = 4\beta d\cos\phi + \alpha = 2\pi(\gamma + 1) = 2\pi\gamma \tag{25}$$

$$\psi_5 = 5\beta d\cos\phi + \alpha = \frac{5\pi}{2}\gamma \tag{26}$$

The total output E can be obtained by adding all vectors of E.

$$\begin{aligned}\vec{E} &= \vec{E}_0(1 + e^{j\psi_1} + e^{j\psi_2} + e^{j\psi_3} + e^{j\psi_4} + \cdots + e^{j\psi_{n-1}}) \\ &= \vec{E}_0[1 + e^{j\frac{\pi}{2}\gamma} + e^{j\pi(\gamma+1)} + e^{j\pi(\frac{3}{2}\gamma+1)} \\ &\quad + e^{j2\pi\gamma} + e^{j\frac{5\pi\gamma}{2}}] \\ &= \vec{E}_0[1 + e^{j\frac{\pi}{2}\gamma}(1 + e^{j(\frac{\pi}{2}\gamma+\pi)} + e^{j(\pi\gamma+1)} + \cdots)]\end{aligned} \tag{27}$$

For simplicity, let $S = (\frac{\pi}{2} + \frac{\pi\Delta f}{2f_0})\cos\phi = \frac{\pi}{2}\gamma$ (28)

and then,

$$\vec{E} = \vec{E}_0(1 + e^{js})\, e^{j\frac{s}{2}(n-2)}\, \frac{\cos\frac{ns}{2}}{\cos s} \tag{29}$$

The magnitude of E yields

$$E = E_0\sqrt{2(1 + \cos s)}\,\frac{\cos\frac{ns}{2}}{\cos s} \tag{30}$$

When $\phi = 0$, from Eq. (27)

$$\begin{aligned}\vec{E} &= \vec{E}_0(1 + je^{j\pi\Delta f/2f_0})(1 + e^{j2\pi\Delta f/2f_0} + e^{j4\pi\Delta f/2f_0} \\ &\quad + \cdots) \\ &= \vec{E}_0(1 + je^{j\pi\Delta f/2f_0})\, e^{j\frac{\pi\Delta f}{2f_0}(\frac{n}{2}-1)} \cdot \frac{\sin(\frac{n\pi\Delta f}{4f_0})}{\sin(\frac{\pi\Delta f}{2f_0})}\end{aligned} \tag{31}$$

The magnitude of E in this case is

$$E = E_0\sqrt{2(1 - \sin\frac{\pi\Delta f}{2f_0})} \cdot \left|\frac{\sin\frac{n\pi\Delta f}{4f_0}}{\sin\frac{\pi\Delta f}{2f_0}}\right| \tag{32}$$

If $\Delta f \ll f_0$,

$$E = nE_0\sqrt{\frac{1 - \sin\frac{\pi\Delta f}{f_0}}{2}} \cdot \left|\frac{\sin\frac{n\pi\Delta f}{4f_0}}{\frac{n\pi\Delta f}{4f_0}}\right| \tag{33}$$

Eq. (33) shows that the output selectivity is still of the $\frac{\sin x}{x}$ form. Comparing Eqs. (33) with (12), the output in the double-electrode transducer is reduced to $\sqrt{\frac{1}{2}}$ of the output in the single-electrode transducer, at the optimum frequency. However, as Δf increases, the amplides of sidelobes decrease as much as $\sqrt{1 - \sin(\pi\Delta f/2f_0)}$ in the double-electrode transducer.

That is the main feature of using double-electrode. Further, we may expect less radiation loss and reflection loss by plotting E vs. ϕ from Eq. (30), similar to the antenna arrays. Simultaneously, driving point impedance is also smaller in the double-electrode type than in the single-electrode type.

Triple-electrode Transducer

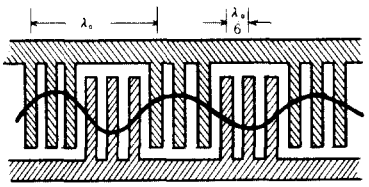

Fig. 6. Triple-electrode transducer.

First evaluate the progressive phase shift.

$$\psi_0 = 0 \tag{34}$$

$$\psi_1 = \beta d\cos\phi + \alpha = \beta\frac{\lambda_0}{6}\cos\phi + 0 = \frac{\pi}{3}\gamma \tag{35}$$

Let

$$R = \frac{\pi}{3}\left(1+\frac{\Delta f}{f_0}\right)\cos\phi = \frac{\pi}{3}\gamma \tag{36}$$

Then

$$\psi_1 = R \tag{37}$$

$$\psi_2 = 2R \tag{38}$$

$$\psi_3 = 3R + \pi \tag{39}$$

$$\psi_4 = 4R + \pi \tag{40}$$

$$\psi_5 = 5R + \pi \tag{41}$$

Therefore, the total output E becomes

$$\vec{E} = \vec{E}_0\left(1 + e^{j\psi_1} + e^{j\psi_2} + e^{j\psi_3} + \cdots\right)$$

$$= E_0\left(1 + e^{jR} + e^{j2R}\right)3^{j\frac{R}{2}(n-3)} \cdot \frac{\cos\frac{nR}{2}}{\cos\frac{3R}{2}} \tag{42}$$

The magnitude of E is also obtained as

$$E = E_0\sqrt{3 + 2\cos\frac{\pi\gamma}{3} + 2\cos\frac{2\pi\gamma}{3}\left(1+\sin\frac{\pi\gamma}{3}\right)\sin\frac{2\gamma}{3}} \cdot \left|\frac{\cos\left(\frac{n\pi\gamma}{6}\right)}{\cos\left(\frac{\pi\sigma}{2}\right)}\right| \tag{43}$$

When $\phi = 0$, from Eq. (41),

$$E = E_0\sqrt{A^2 + B^2} \cdot \left|\frac{\sin\left(\frac{11\pi\Delta f}{6f_0}\right)}{\sin\left(\frac{\pi\Delta f}{2f_0}\right)}\right| \tag{44}$$

where

$$A = 1 + \frac{1}{2}(\cos Q - \cos 2Q) - \frac{\sqrt{3}}{2}(\sin Q + \sin 2Q)$$

$$B = \frac{1}{2}(\sin Q - \sin 2Q) + \frac{\sqrt{3}}{2}(\cos Q + \cos 2Q)$$

$$Q = \frac{\pi\Delta f}{3f_0}$$

It is noted that in the direction of surface-wave reception, the output selectivity is of the form $\frac{\sin x}{x}$ which is required for bandpass filter, as one can be seen from Eq. (44). However, there is a constraint factor inside of square root in Eq. (44) and this factor plays an important role to adjust the amplitudes of side lobes. The main reason to use the triple-electrode transducer is to control the output selectivity and to achieve a chevychev type bandpass response.

Discussions and conclusions

We have analyzed three types of transducers such as single-electrode transducer, double-electrode transducer and triple-electrode transducer, and have investigated the feasibility of fabricating a small-size bandpass filter which is compatible with integrated circuits. The main purpose of this study was first to investigate the characteristics of various types of surface-wave sonic transducer configurations, second to search the utilization of three types of transducers into practice and finally to set up the theoretical criterion in designing surface-wave devices.

As a result, the single-electrode transducer can be used in the signal processing sections and communication systems which frequency domain sidelobe levels smaller than 13.5 db below the passband level are required, and which the main lobe of the output is utilized to a bandpass region and the side lobes to traps because the output response is of the $\frac{\sin nx}{\sin x}$ or $\frac{\sin x}{x}$ form without any constraint function.

Bandpass filters for example are required with frequency domain side lobe levels greater than 60 db below the passband level in combination with shape factors lesss than 2:1. This type of performance has not yet been realized. It may be possible closely to meet such delicate specifications by using the double-electrode transducer and the triple-electrode transducer because the multi-electrode transducer has a main feature of controlling the amplitudes of side lobes.

The optimum frequency is proportional to the wave velocity of the crystal used and inversely proportional to the transducer pitch (Eq. 1). The bandwidth

of the device is inversely proportional to the number of the transducer strips (Eq. 18), and the stability and Q are related to the device dimens Eq. 20). Further, amplitudes, radiation loss, insertion loss, reflection loss and impedances of the surface acoustic devices can be adjusted by choosing various types of transducers.

Further significant developments in the surface acoustic wave devices are expected, due to their unique properties of small sizes, simple fabrication techniques, high reliability, and satisfactory electrical performance for specific applications when compared with alternate techniques.

References

1. J.D. Maines and E.F. Paige, "Surface-Acoustic-Wave Devices for Signal Processing Applications," *Proc. IEEE*, Vol. 64, 1976.
2. B.A. Auld, "Acoustic Fields & Waves in Solids," John Wiley & Sons, Inc., New York, NY 1973.
3. R.M. White and F.W. Voltmer, "Direct Piezoelectric Coupling to Surface Elastic Waves," *Appl. Phys. Left.*, Vol. 7, 1963.
4. C.C. Tseng, "Frequency Response of an Interdigital Transducer for the Excitation of Surface Elestic Waves", *IEEE Trans. Electron Devices*, Vol. ED-15, 1968.
5. B.A. Auld and G.S. Kino, "Normal Mode Theory for Acoustic Waves and its Application to the Interdigital Transducer", *IEE Trnas. Electron Devices*, Vol. ED-18, 1971.
6. P.H. Carr, "Reduction of Reflection in Surface-Wave Delay Lines with Quarter-Wave Taps", *Proc. IEEE*, Vol. 60, 1972.
7. A.K. Gangully and M.O. Vassell, "Frequency Response of Acoustic Surface-Wave Filters," *J. Appl. Phys.*, Vol. 44, 1973.
8. P.N.T. Wells, "Biomedical Ultrasonics", *Academic Press*, New York, NY 1977.
9. Herbert Matthews, "Surface Wave Filters," John Wiley & Sons, Inc., New York, NY 1977.
10. Chang E. Kang, "Electromagnetic Field Theory Approach to SAW Resonators," *71st Annual Symposium of Academy of Science*, Illionis State University, Normal, Illionis, April, 1978.
11. C.S. Hartmann, "Weighting Interdigital Surface Wave Transducers by Selective Withdrawal of Electrodes," *1973 Ultrasonics Symp.*, Proc. IEEE Cat. No. 73CH0807-8SU.
12. H. Engan, "Surface Acoustic Wave Multielectrode Transducer", *IEEE Trans. Sonics & Ultrasonics.*, Vol. SU-22, 1975.
13. G.L. Mattaei, D.Y. Wong and B.P. O'Shaughnessy, "Simplifications for the Analysis of Interdigital Surface Wave Devices", *IEEE Trans. Sonics & Ultrasonics*, Vol. SU-22, 1975.
14. G.L. Mattaei, B.P. O'Shaughnessy and F. Barman, "Relations for Analysis and Design of Surface Wave Resonators", *IEEE Trans. Sonics & Ultrasonics*, Vol. SU-23, 1976.
15. C.M. Pansik and B.J. Hunsinger, "Harmonic Analysis of SAW Transducers, *IEEE Trans. MTT*, Vol. MTT-26, No. 6, 1978.
16. D. Datta and B.J. Hunsinger, "Element Factors for Periodic Transducer", *IEEE Trans. Sonics & Ultrasonics*, Vol. SU-27, No. 1, 1980.
17. R.C.M. Li and J. Melngailis, "The Influence of Stored Energy at Step Discontinuity on the Surface-Wave Gratings," *IEEE Trans. Sonics & Ultrasonics*, Vol. SU-22, 1975.